International Journal of Mathematical, Engineering and Management Sciences
Vol. 11, No. 1, 400-416, 2026
https://doi.org/10.33889/IJMEMS.2026.11.1.017

Modeling and Analysis of Metamaterial-Based Backward Wave Oscillator Using PIC Simulation

Jyoti P. Vengurlekar
Department of Electronics and Telecommunication Engineering,
D Y Patil deemed to be a University, Navi Mumbai, Maharashtra, India.
Corresponding author: jyoti.vengurlekar@rait.ac.in

Bhushan Deore
Department of Electronics and Telecommunication Engineering,
D Y Patil deemed to be a University, Navi Mumbai, Maharashtra, India.
E-mail: bhushan.deore@rait.ac.in

Ayush Saxena
Department of Electrical Engineering,
Veermata Jijabai Technological Institute, Mumbai, Maharashtra, India.
E-mail: ayushsaxena3108@gmail.com

(Received on April 26, 2025; Revised on June 19, 2025 & September 7, 2025 & October 13, 2025;
Accepted on October 23, 2025)

Abstract
The paper presents the modeling and analysis of backward wave oscillators (BWOs) using the MAGIC particle-in-cell (PIC) solver, a high-resolution 2D/3D finite-difference time-domain (FDTD) tool with perfectly matched layer (PML) boundary conditions. A BWO developed at the University of California, Irvine (UCI) is used as a reference model for structural and operational comparison. According to referred model, UCI PIC simulations, this setup generated an output power of 88 MW at 2.9 GHz when driven by a 490-kV electron beam. However, the experimental setup reported an output power of 22 MW at 3.0 GHz. The researchers noted that "the discrepancy with the PIC simulations can be attributed to features in the experiment that deviated from the idealized calculations in the PIC simulations". This observation provides the motivation for the present study.

In current work, metamaterial-based backward wave oscillator is designed using MAGIC PIC simulation setup, results are validated against those presented in the reference paper. The output power of the BWO is investigated under different emission conditions. The results indicate that the idealized simulations and experimental outcomes is likely due to particle emission from the cathode in azimuthal and transverse directions. In oscillators current density and beam quality changes with change in emission modes, it significantly affects beam– wave interaction and overall power efficiency of the devices. A comparative analysis for two different configurations of metamaterial-based high-power microwave oscillator is presented. case 1 which is idealized condition, with an emitting annular cathode that generates output power of 145.24 MW, and case 2, which is replica of realistic conditions, i.e. with an emit-only geometry that generates 16.466 MW—reveals that emission configuration significantly impacts both output power and oscillation frequency. The finding shows that even within simulation environments, emission geometry and alignment play a vital role in output power. Therefore, idealized models may overlook key non-ideal physical effects, reinforcing the importance of incorporating realistic emission conditions in high-power microwave source simulations.

Keywords- Metamaterials, Backward wave oscillators, Particle-in-cell simulation, Electron beam.

1. Introduction

The vacuum electron devices (VEDs) are major sources of generating high-power microwave radiation. These devices rely on the interaction between a relativistic electron beam and an engineered slow-wave structure (SWS) to produce coherent microwave radiation sources. The backward wave oscillator (BWO) is one of the potential high-power microwave devices. BWOs are preferred due to its larger bandwidth.

Optimized design, correct modeling and beam - wave interaction are the important parameters in the improvement of the performance metrics such as output power, efficiency (Luginsland et al., 2022).

Recent experimental and PIC simulation work on metamaterial- based vacuum electron devices (Thakur et al., 2023) show the interest in metamaterials (MTMs) based slow-wave structure for design and modeling of high- power microwave (HPM) radiation sources. The need to incorporate realistic emission models in simulation framework of oscillators has been highlighted by recent physics- based studies of thermionic cathodes, which demonstrate that patch-field effects and surface heterogeneity naturally produce strongly non-uniform emission and affect the transition between temperature- limited and space- charge- limited regions (Chen et al., 2021, 2022). According to recent work, precise modeling of emission and particle statistics is essential for achieving accurate results in experimental devices, and algorithmic and reduced-physics approaches can have a substantial impact on computational predictions of space- charge- limited emission (Evstatiev & Hess, 2023). Our comparison of idealized and realistic emission geometries is further motivated by experimental and PIC simulation studies of cathode emission surface defects, which indicate that localized emission defects or cathode patchiness can change sheath formation and current delivery to the beam, thereby affecting device performance (Chen et al., 2024).

The recent experimental and simulation modeling studies show that consistently cathode emission geometry and non-uniformity to be first-order factors in reconciling PIC predictions with measured experimental HPM device performance. Overall, the conclusion is realistic emission modeling enhances simulation predictability which closely resembles with experimental performance.

The reference model employed is the simulation model of the metamaterial-based backward wave oscillator (BWO) developed at the University of California, Irvine (UCI) (de Alleluia et al., 2020). Artificially structured metamaterials (MTM) have special electromagnetic characteristics. UCI researchers developed an MTM slow wave structure for testing. The UNM SINUS-6 electron beam is used as the input. A 490-kV electron beam was used to drive the MTM SWS; the UCI PIC simulations predicted an output power of 88 MW at 2.9 GHz. The output powers of 22 MW at 3.0 GHz were observed in the experiments. The researchers have reported that “the discrepancy with the PIC simulations can be attributed to features in the experiment that deviated from the idealized calculations in the PIC simulations”. This is the motivation of the current study. The referenced works of de Alleluia et al. (2020), which focused primarily on the structural fabrication and testing of MTM-SWS devices, and Abdelshafy et al. (2021), which centred on dispersion engineering, The current study focuses on the role of electron beam emission profiles in achieving experimental–simulation fidelity, which has not been directly addressed in the literature to our knowledge, and also uniquely emphasizes the impact of emission geometry in PIC simulations and its quantitative comparison with output power performance. Physical experimentation with vacuum electron devices is difficult, in such cases simulation plays an important role. Simulation fidelity is also one of the important factors in the modeling and analysis of HPM devices. PIC is a computational technique used to model the behaviour of charged particles in complex systems. It’s a virtual laboratory setup for modeling and analysis of high-power microwave devices. PIC toolkit demonstrates how several charged particles behave in electromagnetic fields.

Section 1 briefly discusses literature and explains objective of the study, with emphasis on relativistic backward wave oscillators (BWOs) as high-power microwave sources. It describes the goals of the current work and highlights the use of particle-in-cell (PIC) simulations for analysis of high-power microwave devices. Section 2 presents modeling and analysis of the metamaterial-based high- power microwave BWO. It also includes an analysis of the two types of BWO configurations. The case 1 geometry has an annular cathode surface that is described in cylindrical coordinates (z, rho, phi=3.185 rad), while the case 2

geometry is "emit-only" at the same angular position. Subsection 2.1 comprises of metamaterial ring structures and the design and development of the metamaterial-based slow-wave structure. Section 3 of this paper presents the simulation results of both configurations and also includes a comparative analysis of the performance parameters such as output power and frequency. The conclusion outlines the main finding of the research, along with recommendations for future developments in high-power microwave device modeling.

2. Methodology

The metamaterial-based backward wave oscillator (BWO) is a high-power microwave (HPM) radiation source. It operates on the principle of beam-wave interaction guided by metallic waveguide structure, referred as a slow-wave structure (SWS). The current work is employed with metamaterial (MTM) based SWS. MTM is artificially engineered structure, it possesses unique electromagnetic properties. MTM is used to make device compact. A high-current relativistic electron beam interacts with a metamaterial-based periodic structure inside a BWO. It generates coherent microwave radiation. The device operates in the backward- wave mode, in which the electron beam direction is opposite to the generated electromagnetic wave phase velocity (Deshpande et al., 2012; Levush et al., 1996). The performance of two configuration is analyzed with the performance metrics emitted current, collected current and output power using the MAGIC Particle-in-Cell (PIC) simulation framework (Eser et al., 2019).

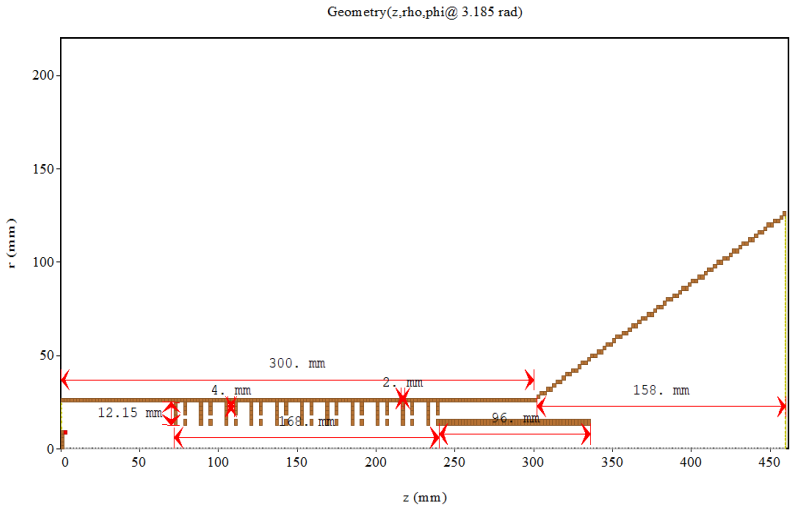

Figure 1. Metamaterial- based backward wave oscillator.

Figure 1 shows the simulated model of the MTM based BWO. The MAGIC PIC simulation setup is used to replicate the BWO design (de Alleluia et al., 2020). The electron beam, annular cathode, metamaterial-based slow- wave structure, collector, horn antenna, and circular waveguide port are the major components of the BWO. The annular cathode is located at the left end of the device (position 0 mm), emits an annular (ring-shaped) electron beam. The emitted electrons are accelerated and directed toward the slow-wave structure (Carter, 2018). The annular electron beam propagates along the z-axis. The beam- wave interaction generates microwaves inside slow wave structure (SWS). SWS is composed of metamaterial unit elements along with the interaction region. The wave slows down at the slow-wave structure (SWS) (Abdelshafy et al., 2021; Chipengo, 2017), which is responsible for effective energy exchange between the electromagnetic wave and the electron beam. This interaction leads to the amplification of microwave radiation. After transferring their energy to the microwaves, the spent electrons are collected at the collector,

which is positioned at the end of the SWS. The horn antenna is used for power extraction. The amplified microwaves are extracted using a horn antenna. A circular waveguide port at the end (450 mm) is used to couple and transport the extracted microwave power. The port ensures minimal reflection and maximum power transmission. The coordinate system in the diagram indicates the z-axis as the primary direction of beam propagation (Klimov, 2013), while the x and y axes represent the transverse directions. The perfectly matched layer (PML) boundary conditions (not shown here) ensure accurate simulation results by preventing artificial reflections at the simulation boundaries.

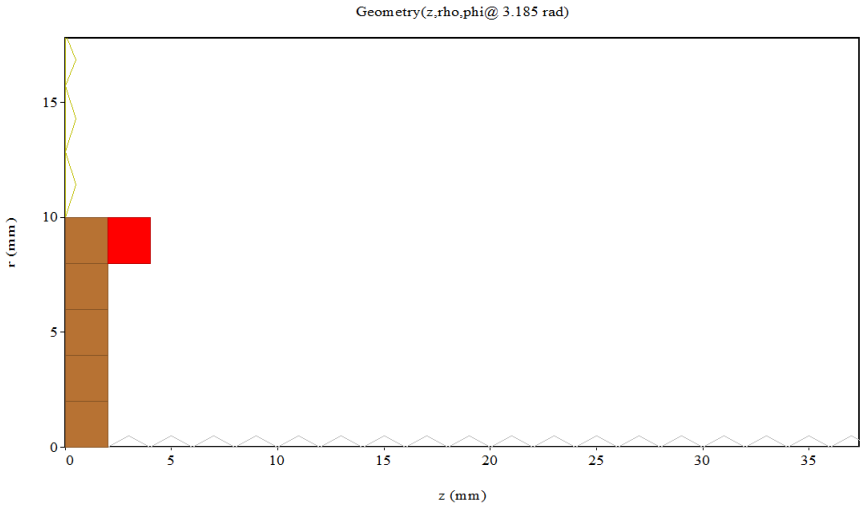

Figure 2. Case 1 geometry (z, rho, phi = 3.185 rad) annular cathode surface.

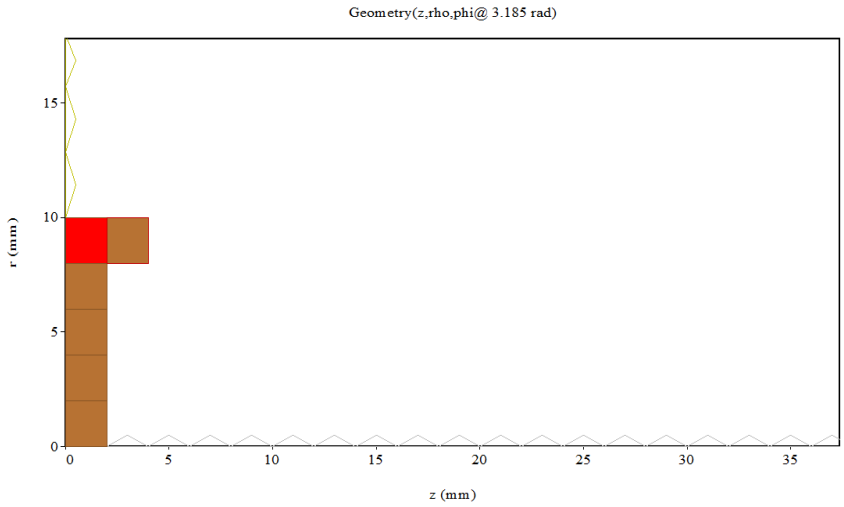

Figure 3. Case 2 only geometry (z, rho, phi = 3.185 rad).

Figures 2 and **3** represent the cathode emission geometry. The (z, rho, phi(φ) = 3.185 rad) cylindrical coordinate system is used in MAGIC simulations (Miller et al., 1998). Here z-axis is the alignment of the electron beam propagation direction and the longitudinal axis of the slow-wave structure (SWS). Rho (ρ) is the radial distance from the central z-axis. Phi(φ) is the azimuthal angle around the z-axis, measured in

radians from a reference direction (typically the x-axis). The marked point is at an azimuthal angle of 3.185 rad, which corresponds to approximately 182.5°. This angle places the point slightly beyond the negative x-axis, effectively just past the mid-plane of the cylindrical geometry. The value of phi (φ) likely relates to field symmetry analysis. To check if the field is mirrored across the position phi (φ) = π or to probe azimuthal variation in field distribution due to MTM loading. The point (z, rho, phi (φ) = 3.185 rad) represents a field probe location used to analyse electric field components Ez, Er and magnetic field component. A field probe location is also used to assess how MTM loading affects field patterns and beam bunching at specific angular positions. Also, mode structures can be analyzed at this diagnostic point, particularly in the case of asymmetric or partial MTM loading, where fields vary with phi φ. In the MAGIC simulation framework, geometry is either fully 3D or exhibits rotational symmetry (2.5D). Such a phi φ specific observation point is crucial for field analysis, mode conversion, asymmetrical MTM SWS, and beam stability in azimuthal direction. **Figures 2** and **3** represent a schematic of both configurations, illustrating the full annular emission in case 1 and the restricted sectoral emission in case 2.

In case 1 (Annular Cathode Surface) configuration, the emission surface is modeled as a continuous annular ring with inner and outer radii corresponding to the physical cathode dimensions. Electrons are emitted uniformly along the entire annular surface, with initial velocities and angular distributions determined by the standard thermionic emission model in MAGIC. In this idealized model, the cathode was defined as a continuous annular surface corresponding to the experimental cathode's physical dimensions. Electrons were emitted uniformly over the full 360° circumference using MAGIC's thermionic emission model, the "idealized" model i.e. case 1 refers to a scenario in which electron emission is prescribed as spatially uniform from a perfectly planar cathode surface, with constant current density and predefined initial beam parameters, independent of local field distributions and cathode surface features. This approach does not account for effects such as cathode curvature, emitter segmentation, or space-charge–limited emission.

In case 2 (Emit-Only Geometry), the segments of the cathode surface that directly face the slow-wave structure (SWS) input section are allowed to emit electrons. The remaining surface elements are treated as non-emitting, thereby replicating the physical shadowing effects and localized emission regions observed in the experimental cathode geometry. This configuration restricts emission to those cathode sectors directly facing the slow-wave structure (SWS) input region, replicating the physical shadowing effects of the experimental assembly. The case 2, refers to "realistic" emission configuration which closely matches with the actual cathode geometry utilized in experiments. This approach enables non-uniform emission and experimental initial velocity spreads, leading to improved alignment between simulations and experimental measurements. Validation of the realistic model was achieved through strong agreement between simulated and experimental microwave output characteristics such as output power and frequency. The case 2 simulation results closely reassemble with the experimental output power (~22 MW) and frequency (~3.0 GHz). Thereby confirming the model's accuracy. The results show that in PIC simulations using realistic conditions for cathode geometry, it significantly improves predictive capability.

In our study, the impact of cathode emission geometry on initial electron velocity and angular distributions is modeled based on the understanding that local electric field variations caused by geometric features on the cathode surface strongly influence electron acceleration directions and velocity spread. The explosive emission model accounts for realistic non-uniform emission patterns caused by micro-protrusions and surface roughness, which generate a broader distribution of emission angles and velocities compared to idealized uniform emission assumptions. While the referred experimental work does not contain direct measurements of these initial electron emission parameters, our simulation approach integrates these physical insights to generate velocity and angular distributions that better reflect the experimental conditions reported in the literature. This allows the PIC simulations to predict macroscopic device

parameters, such as output power and oscillation frequency, in closer agreement with the experimental results. For future work, detailed diagnostic experiments or advanced simulations focusing specifically on initial electron velocity and angular distribution influenced by cathode geometries and explosive emission would be valuable for further quantification.

2.1 Metamaterial-Based Slow Wave Structure (SWS) Design

Metamaterial-based BWO is nothing but a conventional slow wave structure that is replaced by an artificially designed slow wave structure. Metamaterials exhibit unique electromagnetic properties that are not found in natural materials. MTMs are employed to make device compact. The MTM-based SWS utilizes a carefully engineered periodic structure to enhance beam-wave interactions for efficient microwave generation. The MTM- based SWS design, particularly in terms of misaligned irises, improves phase matching between the electromagnetic wave and the electron beam (Marek, 2023). Analysis of these parameters are important for tuning the BWO to optimize device performance and maximize output power and efficiency. The explosive emission model is a type of electron emission that occurs when a high electric field is applied to a cathode. It results in the sudden release of electrons, forming an electron beam. A coaxial waveguide port is placed between the outer surface of the cathode (which emits the electron beam) and the inner surface of the waveguide.

Figure 4. 3-D view of the MTM Slow-Wave Structure (SWS) and waveguide port.

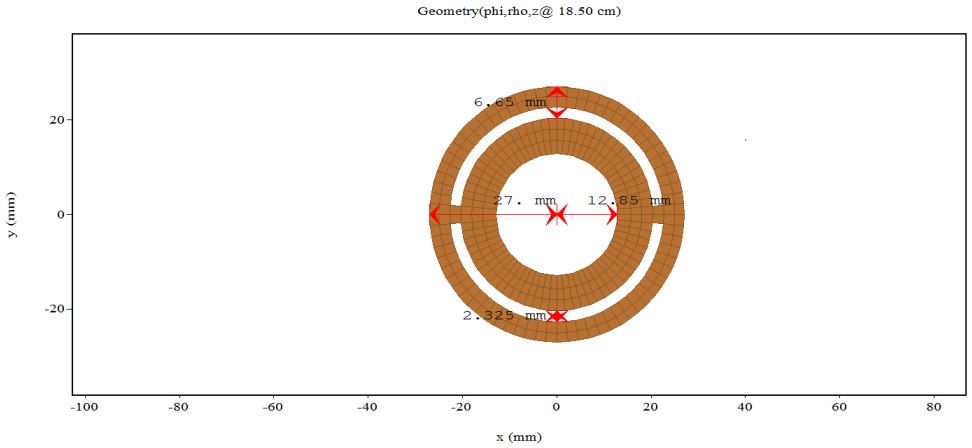

Figure 5. Cross-sectional view of metamaterial structure: metamaterial ring 1.

Figure 4 presents a 3-D view of MTM-SRR showing the inner beam tunnel and the space for electromagnetic wave propagation. This is a disk-loaded circular waveguide structure. It provides a clear

side view of the periodic structure with multiple unit cells along the z-axis. **Figures 5** and **6** illustrate the cross-sectional views of two concentric rings. The fundamental building block, unit cell, of the structure constitutes of two rings are paired together. The unit cell consists of two metallic rings, depending on the length of the slow wave structure, arranged in a periodic pattern. The coordinate system indicates the x, y, and z axes. Irises (narrow openings) are used to control wave propagation and enhance interaction with the electron beam. Iris 1 and Iris 2 have different inner radii r_1 and r_2, contributing to wave dispersion control. The beam tunnel radius, r_b, ensures a clear path for the electron beam. The physical dimensions of the structure are listed comprehensively in **Table 1.**

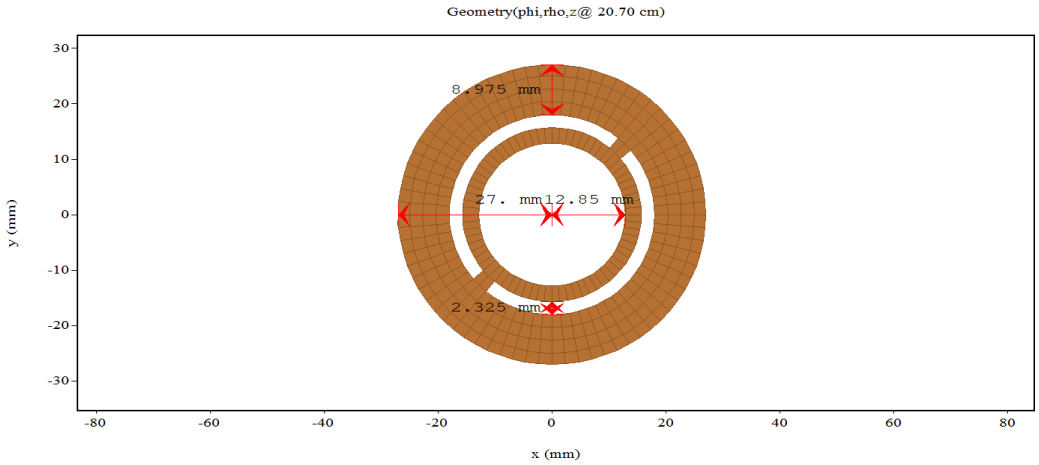

Figure 6. Cross-sectional view of metamaterial structure: metamaterial ring 2.

Table 1 lists the physical dimensions and parameters of the MTM-SWS (Abdelshafy et al., 2021). The outer radius of the circular waveguide is 27mm. Ring separation is the distance between adjacent rings and is 2.325 mm. The inner radius of the first iris is 27mm. The inner radius of the second iris is 21.65mm. The central opening of ring is called beam tunnel radius, is 12.85mm, through which the electron beam passes. The periodic length of one complete unit cell along the z-axis.

Table 1. MTM-SWS parameters and physical measurements.

Quantity	Value
Waveguide radius	27mm
Ring separation	2.325mm
Iris 1 inner radius	27mm
Iris 2 inner radius	21.65mm
Beam tunnel radius	12.85mm
Period	12.15mm

2.3 Simulation Setup

The study utilizes the MAGIC PIC code to investigate the performance of the metamaterial-based backward wave oscillator. MAGIC PIC simulation is a powerful setup for simulating electron beam dynamics and to analyze electromagnetic behavior of charged particles. The explosive emission model is used to capture essential aspects of electron emission from cathode micro-protrusions. The system is driven by high electric fields, but it simplifies complex plasma-surface interactions and temporal emission dynamics. This simplification can affect the exact representation of initial electron velocity and angular distributions, which in turn influence output power and oscillation frequency predictions. Mesh resolution is a critical factor in

accurately resolving local electromagnetic fields and electron trajectories. In our simulations setup mesh resolution was selected to balance accuracy and computational feasibility, it may not fully capture all fine-scale variations, potentially introducing discrepancies when comparing with experimental results. These factors should be considered when interpreting simulation outcomes. The experimental data presented by de Alleluia et al. (2020) provide a valuable benchmark that guides our modeling improvements.

The simulations were conducted using a mesh size of dr = dz = 2mm and an azimuthal segmentation of $d\phi = 2\pi/72$, ensuring adequate spatial resolution for field and particle interactions. The Maxwell High-Q solver was used to set the simulation time step to Magic simulation time parameter. Each cell in the computational domain contained one particle. To maintain stability the particle-to-field time step ratio was maintained at unity. An explosive emission model was used for the cathode, where electron emission was triggered when the local electric field exceeded a threshold value. The electric field threshold is set at 2×10^6 V/cm. This setup provides a practical balance between computational efficiency and physical accuracy for modeling emission-driven beam formation in the backward wave oscillator configuration. While output power is a critical metric and the primary focus of our current validation against the experimental results reported by de Alleluia et al. (2020), several other simulation aspects can and should be further compared with experimental data to enhance validity. Future work will aim to refine both emission models and mesh granularity to enhance simulation fidelity and predictive capability.

3. Results and Discussion

A replica of simulated high-voltage KALI pulse of approximately 550V (Banerjee et al., 2020; Reddy et al., 2019) is used as the input electron beam for a duration of ~20 nanoseconds. The simulated magnetic field is of ~0.5T (Banerjee et al., 2020). The explosive emission model is used to simulate the plasma formation on the material surface inside MTM-SWS due to electric field enhancement at the micro-protrusions of MTM-SWS. This surface plasmon typically emits under the influence of the ambient electric field. In our simulations, the electron beam originates from the cathode surface and propagates along the SWS. The electron beam originating from the cathode inside the BWO is visible in **Figures 2** and **3**. The output power obtained in case 1 is ~165 MW, and in case 2 power is ~16.46 MW. The corresponding FFT of the output microwave power is shown in **Figures 16** and **15** respectively. The output power obtained in case 2 is closer to the referenced experimental output power (de Alleluia et al., 2020). The simulated peak current values are shown in **Figures 9** and **10**. The peak current values are approximately 3.8 kA for case 1 at 2.66 GHz and 3.9 kA for case 2 at 3.7242 GHz. **Table 2** shows some of the input and output parameters.

The experimental magnetic field with a peak value of ~0.5T is not constant and changes along the longitudinal axis (z). Hence, to replicate the same, the magnetic field profile is obtained by fitting the experimental magnetic field data with a 5th-order polynomial, which results in a spatial function in terms of the z-coordinate, and hence, can be passed in the PIC code (Banerjee et al., 2020; Reddy et al., 2019).

The emitted current is not directly controlled but instead depends on the emission model in the simulation. This means the current value results from how the electrons are emitted under the applied voltage. At the end of the metamaterial-based SWS, a metallic cylinder is placed. This cylinder acts as a beam collector with a radius equal to the beam tunnel radius (rb). Its purpose is to capture stray electrons, preventing them from reaching the output port, which could interfere with the microwave output. The generated microwaves are extracted using a horn antenna (Abdallah et al., 2000).

Figure 7 (Emitted ALL CURRENT vs. Time (case 1 vs. case 2)) displays the total emitted beam current

for both geometries measured 3 mm from the cathode surface (case 2 in blue, case 1 in red). In this ALL CURRENT represents total current emitted from the cathode region, possibly this is calculated over the entire electron emission surface. Current is measured in kiloamperes (kA), and time is measured in nanoseconds (ns). This current includes the primary beam current emitted into the SWS beam- wave interaction region and back- travelling or reflected components current. Again, the value depends on how simulation tool defines this context. The simulation uses the m3d format to track time -dependent or steady -state behavior of the emitted beam current. The case 1 curve of current indicates more stable current output reflects a higher emission rate, and possible modulation effects if oscillations are observed. Since this is Emitted ALL CURRENT on ALL, includes total cathode area current, without filtering for specific beamlets or phase spaces. Current emission characteristics can be determined by considering the oscillation patterns, rising slopes, and peak values of the emitted current curves.

Figure 8 (Collected ALL CURRENT vs. Time at Collector Surface) represents the total beam current collected at the output port for both configurations. Time duration is in nanoseconds shown on x axis and current (kA) is plotted on the y axis. The electron beam is emitted from the cathode, interacts with the MTM-based SWS, and then travels toward the collector. The "Collected ALL CURRENT on ALL" plot shows how much beam successfully exits the interaction region and is absorbed at the collector. This is a major diagnostic parameter for the analysis of beam transport efficiency, identifying loss mechanisms, and verifying collector design performance. It represents the total current absorbed by the collector surfaces after beam–wave interaction in the metamaterial slow-wave structure. If high amount of current is collected it means that there is a good beam guidance in SWS, low interception losses, and indicates appropriate collector design. Beam instability, space charge effects causing beam spreading or interception could indicate few of the causes for drop in collected current over time.

The time-domain data is extracted from the **Figure 8**. Then FFT is plotted for the individual configuration namely case 1 and case 2. The frequency spectrum of the collected current signal is shown in **Figures 9** and **10**. Frequency (GHz) is on the x-axis, magnitude (normalized units or dB) on the y-axis. A single dominant peak indicates stable beam–wave interaction. **Figure 9** represents a 2.6601 kA current around 2.6 GHz in case 1 configuration, whereas **Figure 10** represents 3.7242 kA current around 3.8 GHz in case 2 configuration. Peak power near 3.72 GHz indicates modified beam dynamics due to emission geometry.

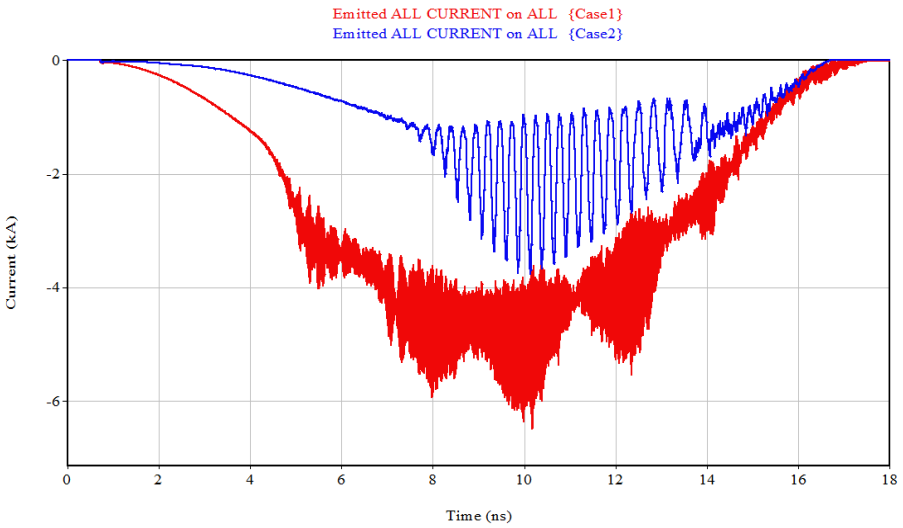

Figure 7. Emitted ALL CURRENT on ALL {BWO 50mm2_8double_Emittonly.m3d}.

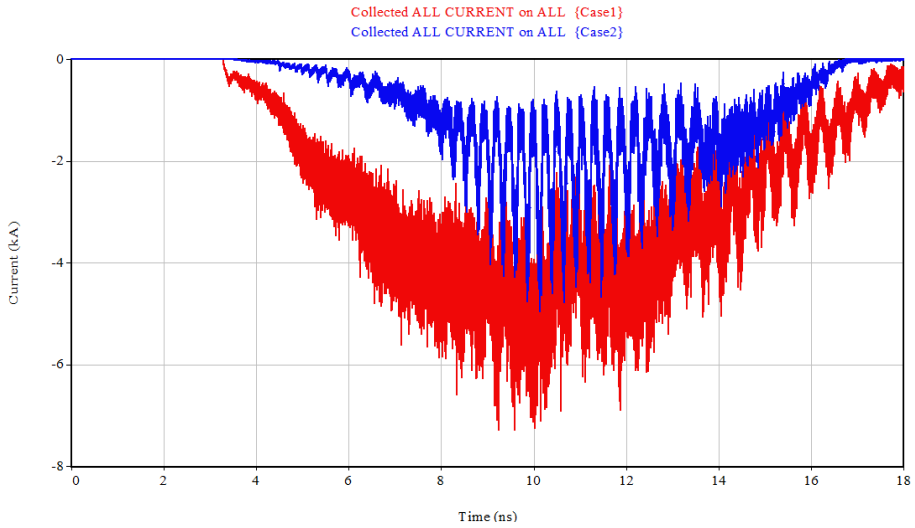

Figure 8. Collected ALL CURRENT on ALL.

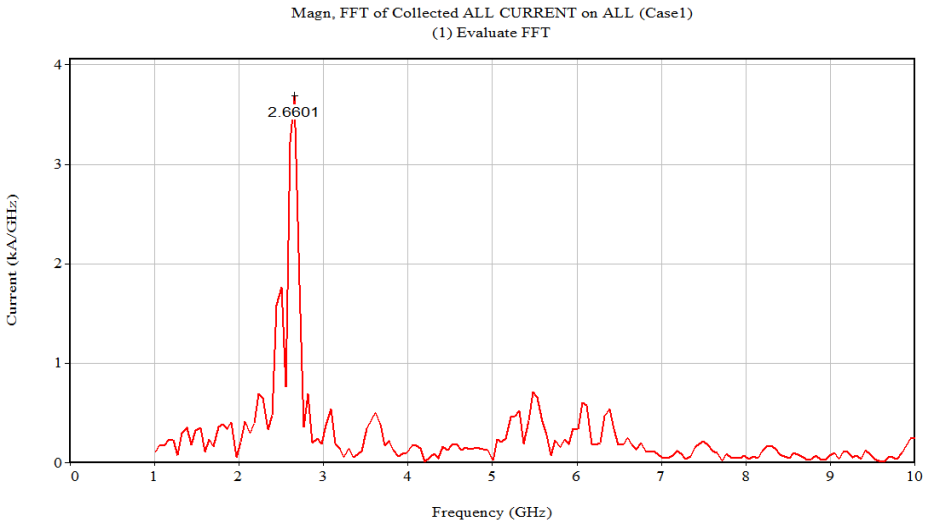

Figure 9. FFT of Collected ALL Current – case 1.

To examine efficiency of MTM-loaded BWO, we have to examine power flow from two complementary perspectives: where the energy originates and where it is delivered. **Figures 11** and **12** illustrate this dynamic through two critical diagnostics in the MAGIC simulation: Power E.J_PARTICLE.DV and Power S.DA. Though both relate to power calculations, they originate from fundamentally different physical mechanisms, each capturing a different aspect of the beam–wave interaction. The PIC simulations' waveforms help to analyze how efficiently the beam is generated and how it behaves over time.

Figure 11 displays the electromagnetic signal detected at the waveguide port i.e., the horn's aperture. There is a noticeable 5 ns delay after applying the beam pulse till detection of the radio frequency output pulse. This delay is caused by the time it takes for the electromagnetic wave to travel through the slow-wave

structure and reach the horn antenna. Power (E·J) vs Time, represents instantaneous power transfer from the electron beam to the RF field. It uses the dot product of electric field (E) and current density (J) (Matos et al., 2006). Power (MW) is plotted against time (ns). This theoretical analysis shows the energy transfer efficiency. It is calculated using volume integral of the electric field vector (E) and the particle current density vector (J_particle) dot product (Capps, 2017):

$$\text{Power} = \int_V \vec{E} \cdot \vec{J}_{\text{particle}}\, dV \quad (1)$$

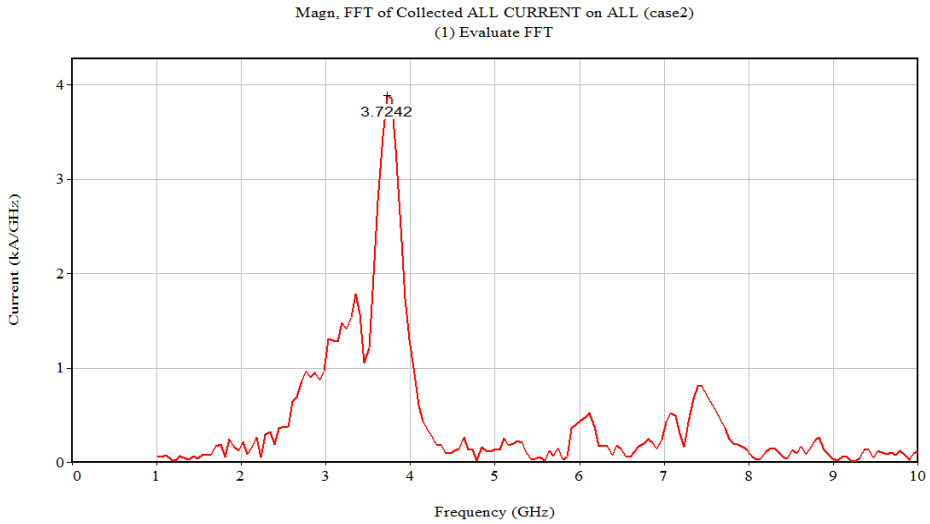

Figure 10. FFT of Collected ALL Current – case 2.

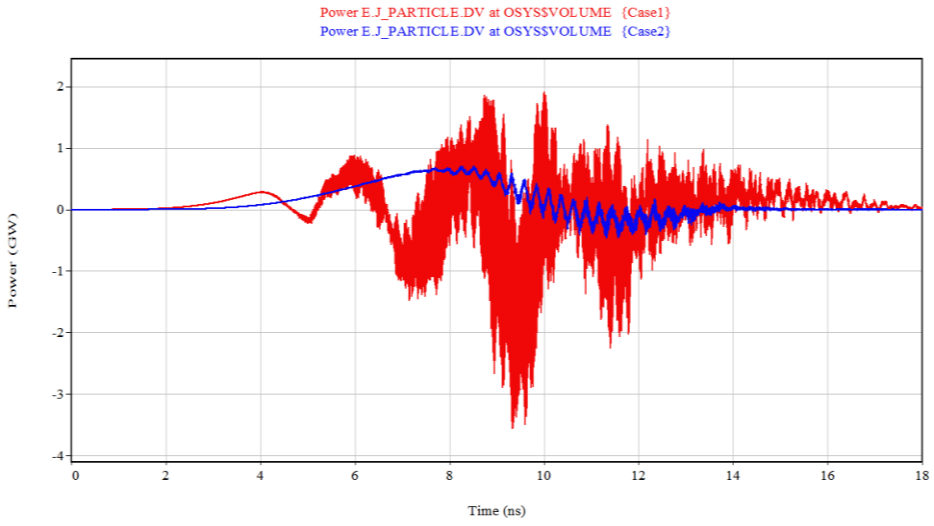

Figure 11. Power E.J_PARTICLE.DV at OSYS$VOLUME.

This parameter measures the work done by the electron beam on the electromagnetic fields, indicating how much energy the beam is transferred into the wave. This provides an important measurement of internal energy exchange responsible for oscillation and amplification inside BWO. Positive values imply that

energy is being transferred from the beam to the RF wave, which is the desired condition during normal BWO operation (Hegeler et al., 2000). Negative values suggest energy is flowing from the wave back to the beam, which can occur in cases of wave reflection, beam–wave mismatch, or saturation. The Power E.J_PARTICLE.DV diagnostic is computed from volume-based field and particle data inside the simulation domain and is especially useful for identifying where and how strongly the beam is exciting RF fields. As shown in **Figure 11**, this helps assess the spatial distribution and efficiency of energy transfer. While E.J_PARTICLE.DV measures localized energy transfer from particles to fields, and Power S.DA captures net electromagnetic power flow through surfaces. **Figure 12** Power S.DA at Output Port, case 1 displays RF power flow (MW) at the waveguide output using the surface integral of the Poynting vector. Time (ns) is on the x-axis, power (MW) on the y-axis.

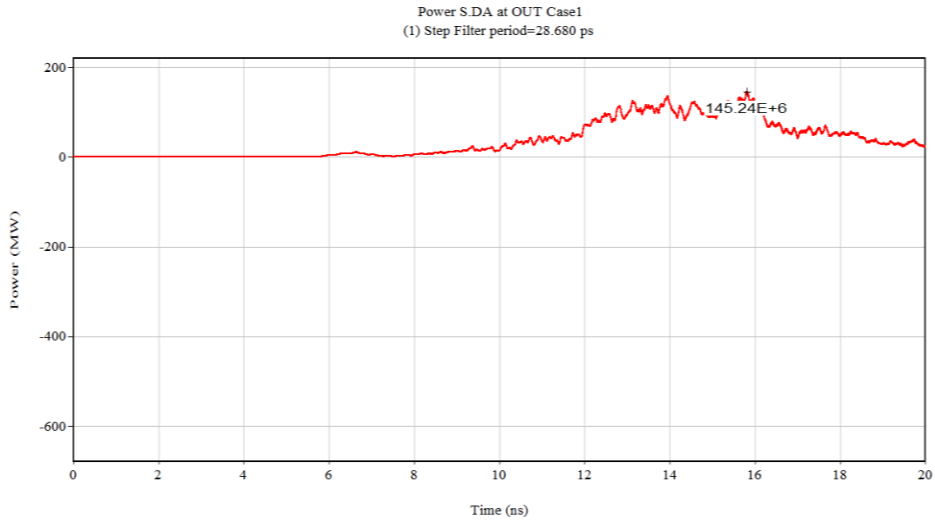

Figure 12. Power S.DA at OUT case 1.

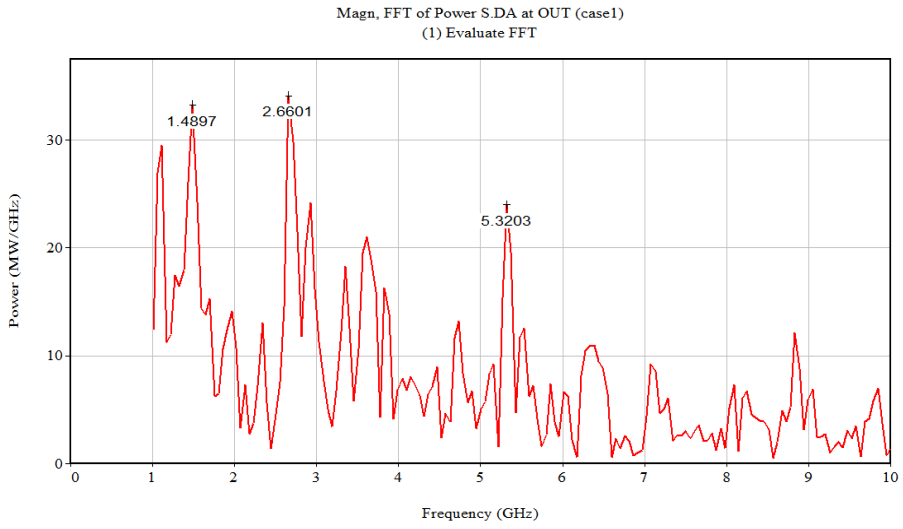

Figure 13. Magnitude, FFT of power S.DA at OUT (case 1).

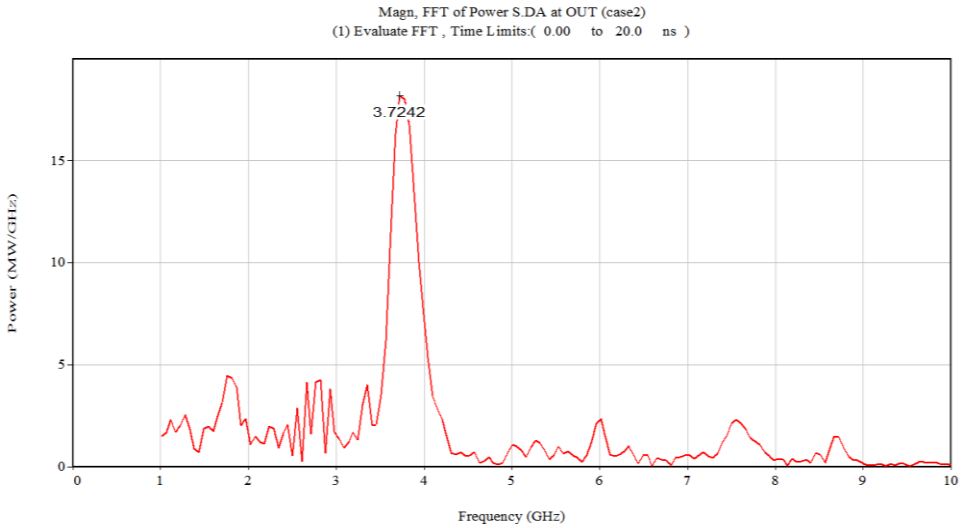

Figure 14. Magn, FFT of Power S.DA at OUT (case 2).

Figures 13 and **14** are the Fast Fourier Transform (FFT) applied to the output power signal. The FFT is a mathematical technique used to convert a time-domain signal (e.g., power vs. time) into its frequency components (e.g., power vs. frequency). Power S.DA likely represents the Signal Data Analysis (S.DA) of the output power at a specific monitor or port, often located at the horn antenna or waveguide output in the BWO simulation. OUT refers to the location where the power is being monitored, typically the output port where the microwave signal is extracted.

Figures 13 and **14**, shows the FFT on Power S.DA for case 1 and case 2, the X-axis (Frequency) displays the microwave frequency in GHz (typically), and the Y-axis (Magnitude) represents the magnitude of the power at each frequency component, usually in dB or normalized units. FFT resolution is 10 MHz; Total window length is 20 ns. The primary purpose of performing an FFT on Power S.DA is to analyze the frequency spectrum of the generated microwave signal, which is useful for the dominant frequency spectrum analysis. It also shows the desired operating microwave frequency of the BWO. FFT helps in identifying frequency spectrum accuracy. In case 1 configuration, the peak output power is observed at 2.6601 GHz, while in case 2, peak output power is observed at 3.7242 GHz. The sharpest peak on the FFT spectrum is used to identify the oscillation mode (Song et al., 2013). Differences in cathode emission geometry results in frequency change. This is responsible for modification of the initial beam parameters, emission profile, current density distribution, and beam impedance. These changes affect space- charge dynamics and beam– wave interaction efficiency within the slow-wave structure. Multiple peaks, broad spectral spread, or irregular components suggest multimode operation, beam misalignment, or nonlinear effects, which can degrade efficiency and spectral purity (Chipengo, 2017).

Figure 15 presents case 2 - Power S.DA in the time domain and for case 1, Power S.DA in the time domain is presented in **Figure 16**. Power S.DA presents the electromagnetic power flux through the waveguide face, a typical output surface. It is obtained by as the surface integral of the Poynting vector $S = E \times H$, where, E and H are the electric and magnetic fields, respectively (Shore et al., 1997). This parameter measures the net Radio Frequency (RF) power exiting the device, which directly relates to output power efficiency, mode coupling effectiveness, and spectrum purity. In E.J_PARTICLE.DV, volume-based diagnostics, which measures internal energy transfer between beam and fields, Power S.DA focuses on the

deliverable RF power available to a load or antenna. TM_{01} transverse magnetic mode is dominant output mode, a commonly used mode in high-power microwave systems due to its high energy-carrying capacity. **Figures 15** and **16** shows the microwave output power for both configurations. The results show the powerful impact of cathode geometry on frequency stability, mode purity, and overall efficiency performance.

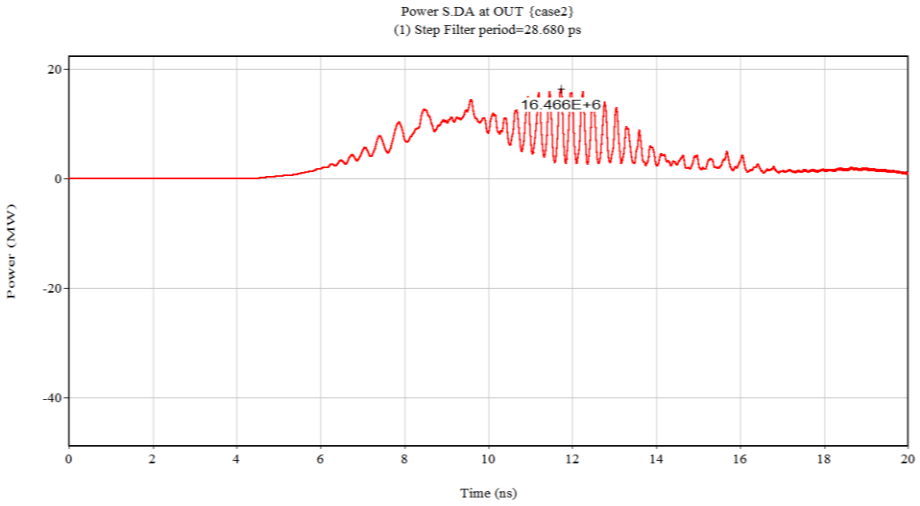

Figure 15. Power S.DA at OUT case 2.

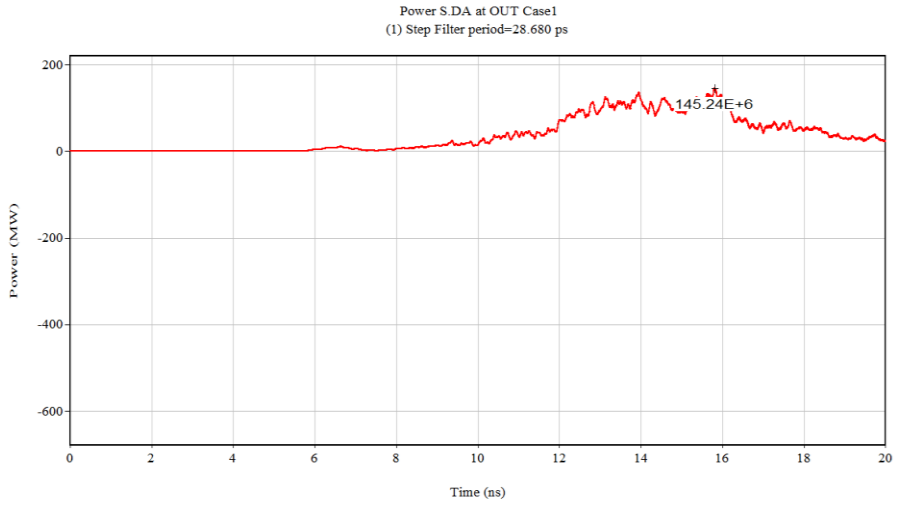

Figure 16. Power S.DA at OUT (case 1).

Table 2. Results.

	Case 1: annular cathode surface	Case 2: emit only geometry
Collected current	3.8 kA at 2.6601 GHz	3.9 kA at 3.7242 GHz
Output power	145.24 MW	16.466 MW

The primary purpose of this study is to model a metamaterial based HPM BWO and then validate this model with existing experimental and simulation results. Further we have analysed different geometries to investigate output power. Overall, the paper presents two distinct cathode emission configurations using MAGIC particle-in-cell simulations. As shown in **Table 2**, case 2- realistic modeling of the emission geometry configured with the factors such as non-uniform emission and surface irregularities—leads to predicted output power of 16.466 MW. In case 1- idealized, uniform emission models the output power is very high compared to case 2. The case 2 configuration brings the simulation results into closer agreement with the experimental observations reported by de Alleluia et al. (2020). This comparative analysis validates the model accuracy. In essence, our work shows that the emission geometry is an important factor in the electron beam formation and interaction with the slow wave structure. It directly affects the output power and oscillation frequency. The output power, frequency stability results show good quantitative agreement. Significantly, the physical geometry in the simulation device remains same as that of referred paper, the design was not drastically changed from the experimental device (de Alleluia et al. 2020). Our contribution lies in increased simulation fidelity through increased modeling of interaction physics and physical operating conditions.

4. Conclusion

This study utilized the MAGIC particle- in- cell (PIC) simulation framework to analyze metamaterial based high-power microwave backward wave oscillator (BWO) performance, referencing the University of California, Irvine (UCI) BWO design for structural and operational validation. The UCI PIC simulations in the referred work reported 88 MW at 2.9 GHz, 490 kV electron beam is used as the input, whereas experimental measurements achieved 22 MW at 3.0 GHz, shows the gap between simulated modeling and experimental modeling performance.

This study presents a modeling and analysis of metamaterial based HPM BWO. Our investigation compared two cathode emission configurations. case 1, with an annular emitting surface, produced 145.24 MW at 2.6601 GHz, while case 2, using a localized emit-only geometry, generated 16.466 MW at 3.7242 GHz. case 1 resembles with the idealized condition which is due to ideal simulation environment whereas case 2 is with realistic emission geometry. The results show that emission geometry strongly affects current density, beam quality, and beam – wave coupling efficiency. Emission in azimuthal and transverse directions plays important role in performance metrics. Emission geometry affects output power and oscillation frequency results in both configurations. The localized emit- only case 2 configuration is closely resemblance with physical setup whereas case 1 resembles with the idealized emission condition.

Overall, the findings indicate that while idealized PIC models provide reference metric. The possible solution to bridge the gap between situational and experimental values is to incorporate realistic emission profiles and geometries. These enables more accurate design and optimization of high-power microwave radiation sources.

Conflicts of Interest

The authors hereby confirm that there is no conflict of interest to declare for above paper.

Acknowledgments

This research has not received any funding agencies in the public, commercial, or not-for-profit sectors grant.

AI Disclosure

During the preparation of this work the author(s) used generative AI in order to improve the language of the article. After using this tool/service, the author(s) reviewed and edited the content as needed and take(s) full responsibility for the content of the publication.

References

Abdelshafy, A.F.A. (2021). *Dispersion engineering of microwave and high-power devices with exceptional points of degeneracy.* Doctoral dissertation, University of California, Irvine. ProQuest Dissertations & Theses Global. 28864513.

Banerjee, T.S., Saxena, A., Hadap, A., Reddy, K.T.V., & Roy, A. (2020). Particle-in-cell simulation of a RBWO with experimental voltage input pulse and external magnetic field. *Physics Open, 3*, 100015. https://doi.org/10.1016/j.physo.2020.100015.

Capps, D.M. (2017). Study of a reflection grating used in Littrow mount. *Applied Optics, 56*(12), 3293-3302. https://doi.org/10.1364/AO.56.003293.

Carter, R.G. (2018). *Microwave and RF vacuum electronic power sources.* Cambridge University Press. ISBN: 9780511979231. https://doi.org/10.1017/9780511979231.

Chen, D., Jacobs, R., Morgan, D., & Booske, J. (2021). Impact of nonuniform thermionic emission on the transition behavior between temperature- and space-charge-limited emission. *IEEE Transactions on Electron Devices*, *68*(7), 3576-3581. https://doi.org/10.1109/TED.2021.3079876.

Chen, D., Jacobs, R., Petillo, J., Vlahos, V., Jensen, K.L., Morgan, D., & Booske, J. (2022). Physics-based model for nonuniform thermionic electron emission from polycrystalline cathodes. *Physical Review Applied, 18*(5), 054010. https://doi.org/10.1103/PhysRevApplied.18.054010.

Chen, T., Li, T., Li, H., Wang, H., Cheng, R., Zhou, H., Hu, B., & Fu, H. (2024). Study of cathode emission surface defects in relativistic magnetrons. *Physics of Plasmas, 31*(2), 023502. https://doi.org/10.1063/5.0188188.

Chipengo, U. (2017). *Novel concepts for slow wave structures used in high power backward wave oscillators*. Doctoral dissertation, Ohio State University. OhioLINK Electronic Theses and Dissertations Center. http://rave.ohiolink.edu/etdc/view?acc_num=osu1499346841806681.

de Alleluia, A.B., Abdelshafy, A.F., Ragulis, P., Kuskov, A., Andreev, D., Othman, M.A.K., Martinez-Hernandez, B., Schamiloglu, E., Figotin, A., & Capolino, F. (2020). Experimental testing of a 3-D-printed metamaterial slow wave structure for high-power microwave generation. *IEEE Transactions on Plasma Science, 48*(12), 4356-4364. https://doi.org/10.1109/TPS.2020.3021041.

Deshpande, P. (2012). The study of Cerenkov cyclotron interaction as a result of passage of intense relativistic electron beam through slow wave structure (Doctoral dissertation, Devi Ahilya Vishwavidyalaya). ProQuest Dissertations & Theses Global. (27531508)

Eser, D. (2019). *Analysis and design of slow wave structure for backward wave oscillators*. Master's thesis, Middle East Technical University (Turkey). ProQuest Dissertations & Theses. *Graduate School of Natural and Applied Sciences of Middle East Technical University*. 31671898.

Evstatiev, E.G., & Hess, M.H. (2023). Efficient kinetic particle simulations of space charge limited emission in magnetically insulated transmission lines using reduced physics models. *Physical Review Accelerators and Beams, 26*, 090403. https://doi.org/10.1103/PhysRevAccelBeams.26.090403.

Hegeler, F., Partridge, M.D., Schamiloglu, E. & Abdallah, C.T. (2000). Studies of relativistic backward-wave oscillator operation in the cross-excitation regime. *IEEE Transactions on Plasma Science, 28*(3), 567-575. https://doi.org/10.1109/27.887675.

Klimov, V. (2013). *Nanoplasmonics* (1st edition). Jenny Stanford Publishing, New York. ISBN: 9780429070488. https://doi.org/10.1201/b15442.

Levush, B., Antonsen, T.M., Vlasov, A.N., Nusinovich, G.S., Miller, S.M., Carmel, Y., Granatstein, V.L., Destler, W.W., Bromborsky, A., Schlesiger, C., Abe, D.K., & Ludeking, L. (1996). High-efficiency relativistic backward wave oscillator: theory and design. *IEEE Transactions on Plasma Science, 24*(3), 843-851. https://doi.org/10.1109/27.533087.

Luginsland, J., Marshall, J.A., Nachman, A., & Schamiloglu, E. (2022). *High power microwave sources and technologies using metamaterials*. Wiley. ISBN: 9781119384441(p), 9781119384472(e). https://doi.org/10.1002/9781119384472.

Marek, A. (2023). *New type of sub-THz oscillator and amplifier systems based on helical-type gyro-TWTs*. Karlsruhe Institute of Technology. ISBN: 978-3-7315-1250-9. https://doi.org/10.5445/KSP/1000151835.

Matos, L., Mücke, O.D., Chen, J., & Kärtner, F.X. (2006). Carrier-envelope phase dynamics and noise analysis in octave-spanning Ti: sapphire lasers. *Optics Express, 14*(6), 2497-2511. https://doi.org/10.1364/oe.14.002497.

Miller, S.M., Antonsen, T.M., & Levush, B. (1998). Ponderomotive effects in plasma-filled backward-wave oscillators. *IEEE Transactions on Plasma Science, 26*(3), 680-692. https://doi.org/10.1109/27.700805.

Reddy, V.V., Ansari, M.A., & Thottappan, M. (2019). Simulation studies of an overmoded RBWO under a low guiding magnetic field. In *2019 IEEE Asia-Pacific Microwave Conference* (pp. 1253-1255). Singapore. https://doi.org/10.1109/apmc46564.2019.9038277.

Shore, B.W., Li, L., & Feit, M.D. (1997). Poynting vectors and electric field distributions in simple dielectric gratings. *Journal of Modern Optics, 44*(1), 69-81. https://doi.org/10.1080/09500349708232900.

Song, W., Zhang, X., Chen, C., Sun, J., & Song, Z. (2013). Enhancing frequency-tuning ability of an improved relativistic backward-wave oscillator. *IEEE Transactions on Electron Devices, 60*(1), 494-497. https://doi.org/10.1109/TED.2012.2230400.

Thakur, A.S., Rawat, M., & Kartikeyan, M.V. (2023). Design of an oppositely-oriented circular split-ring resonator-loaded multibeam all-metallic metamaterial backward-wave oscillator. *IEEE Transactions on Plasma Science, 51*(9), 2625-2631. https://doi.org/10.1109/TPS.2023.3305563.